An Overview of the Recent Advances in FBG-Assisted Phase-Sensitive OTDR Technique and its Applications

Kivilcim Yüksel[1]*, Johan Jason[2], Ertunga B. Kocal[1], Manuel Lopez-Amo Sainz[3], and Marc Wuilpart[2]

[1] *Electronics Engineering Department, Izmir Institute of Technology, Izmir, Turkey*

[2] *Electromagnetism and Telecommunication Department, Faculty of Engineering, University of Mons, Mons, Belgium*

[3] *Electrical and Electronics Engineering Department, Public University of Navarra, Arrosadia Campus, Pamplona, Spain*

Tel: (90) 232.7506540, e-mail: kivilcimyuksel@iyte.edu.tr

ABSTRACT

In this paper, we discuss the operation principles, sensing mechanism, challenges and application areas of FBG-assisted phase-sensitive optical time-domain reflectometry. A special emphasis is given to the interrogation of fiber Bragg grating arrays for vibration sensing application. Results obtained by different research groups are compared in terms of performance characteristics and future perspectives. Recent progress obtained through our research collaboration are also presented. In particular, the detrimental spectral shadowing effect and multiple reflection crosstalk are analysed and mitigation techniques are proposed.

Keywords: phase-OTDR, FBG, optical reflectometry, fiber optic sensors, distributed vibration sensing.

1. INTRODUCTION

Distributed optical fiber sensing (DOFS) was developed more than 20 years ago as a powerful group of alternative technologies to the conventional sensors and since then, many successful applications have been realised across multiple sectors such as oil & gas (i.e. well and pipeline monitoring), manufacturing, energy, transportation, aerospace, security, and the medical sector [1]. These sensors make use of the intrinsic scattering mechanisms (i.e. Raman, Brillouin, and Rayleigh) in single mode fiber (SMF), hence benefit from all the advantages of optical fiber technology (low-weight, small dimensions and immunity to electromagnetic interference).

The Rayleigh backscattering signal (RBS), the primary source of attenuation in optical fiber, has been advantageously exploited for the realization of various distributed sensing systems [2]. Among them, distributed acoustic sensing (DAS) or distributed vibration sensing (DVS), has become the dominant application area that has been experiencing the fastest transition into commercialization. This sensor family relies on the fact that the intensity and phase of the Rayleigh backscattered light vary in response to external perturbations (through strain-optic effect). Most of the interrogation units implemented for DAS/DVS are based on the use of Phase-sensitive Optical Time Domain Reflectometry (ϕ-OTDR), sometimes referred to as Coherent OTDR, in which coherent optical pulses (from a narrow linewidth laser) are launched into the sensing fiber to perform spatially-resolved measurements of RBS.

ϕ-OTDR schemes can be divided into two main categories according to the detection method employed; namely, direct detection and coherent detection ϕ-OTDR. The former approach relies on the measurement of RBS power over time, limited to the fact that the strain transfer function between the magnitude of the vibration and the backscattering signal power is not linear, whereas the latter adopts the coherent detection scheme to extract the *phase* component of the RBS. The knowledge of the phase is particularly important for the *quantification* purpose as it can be used to deduce not only the frequency but also the *magnitude* of external vibrations (i.e. the output of the phase-extracted DAS is linear to the vibration magnitude and is therefore preferred in many industrial applications).

Despite its low SNR, the relatively simple direct detection ϕ-OTDR found a straightforward place in intrusion detection applications [3]. On the coherent ϕ-OTDR side, many schemes (using heterodyne detection [4], digital coherent detection [5,6], self-mixing demodulation [7], dual-heterodyne detection [8], imbalanced Mach-Zehnder interferometer (IMZI) and 3×3 coupler [9], dual-pulse heterodyne system [10], and two-wavelength probe [11]) have been investigated, providing phase demodulation and also featuring an improved SNR.

Even though DAS systems have been successfully demonstrated in many fields, there is still need for further sensitivity improvement due to three factors. Firstly, RBS process has inherently weak signal levels (optical amplification of RBS is limited by nonlinear threshold values of standard telecom-grade fiber). Secondly, polarization and interference fading severely degrade the performance of ϕ-OTDR. Thirdly, the variety of applications of different nature may require different, application-specific ways of enhancing the signal in order to extract the desired information with an acceptable SNR. In that sense, a suitable denoising and signal processing method may be borrowed and adapted to an envisaged application having a set of particular requirements (e.g. a particular vibration frequency range, or a special kind of background noise).

978-1-7281-8423-4/20/$31.00 ©2020 IEEE

The methods proposed in the literature include (but are not limited to); separate and moving averaging method [4], wavelet de-noising method [12], Sobel operators [13], use of dual-pulse phase modulated probe [14], Fourier transform method [15], Hilbert-Huang transform method [16], adaptive filtering [17], phase-shifted double pulse method [18], use of chirped-pulse [19], spectrum extraction and remix (SERM) method [20], and least mean square error (LMSE) adaptive filter algorithm [21]. All these efforts, each with their different complexity, cost, and computational load, can be categorized as enhancement methods at the interrogator side.

Recently, an alternative approach brought about a new paradigm for the sensitivity improvement in DAS. It proposes modifying the sensing fiber itself to obtain a better SNR, rather than enhancing the interrogator and its signal processing stages. Fiber modification can be realized in either a distributed [22-27] or a quasi-distributed manner [28-45]. Figure 1 summarizes two trends in creating a more sensitive fiber that have been published in the scientific literature. The remaining of this paper handles the specific group that is based on the weak fiber Bragg gratings of this classification.

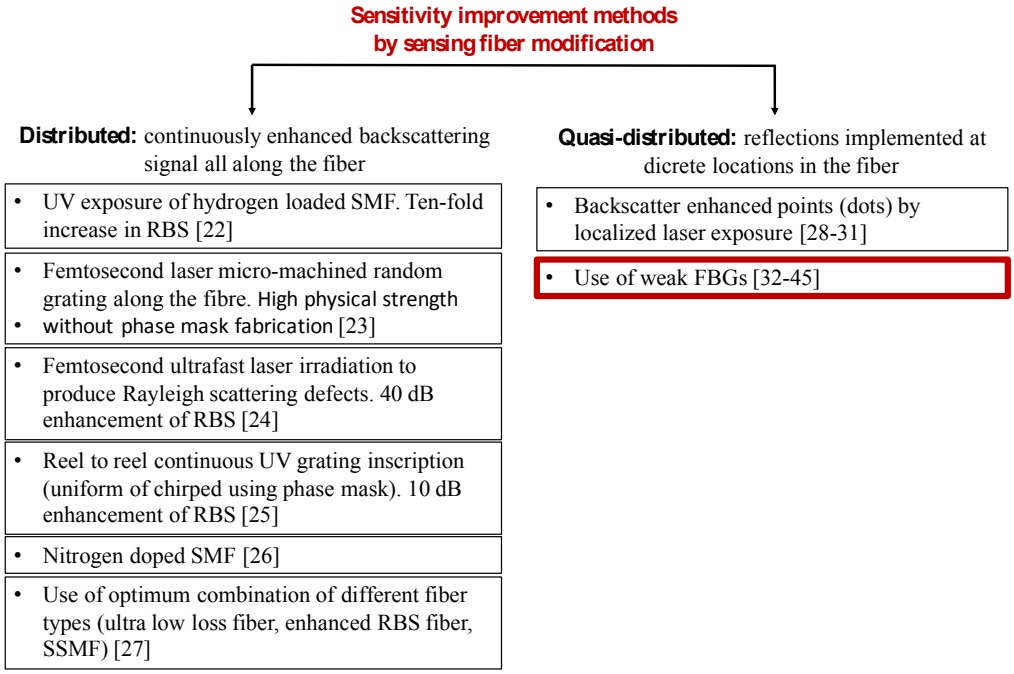

Figure 1. Summary of recent trends in sensitivity improvement methods applied on the sensing fiber.

2. IMPROVED Φ-OTDR SENSING SYSTEMS BASED ON FIBER BRAGG GRATING ARRAY

Signal-to-noise-ratio (SNR) improvement and elimination of fading noise are of critical importance to provide high-precision dynamic strain measurement capability. The use of fiber Bragg grating (FBG) arrays to improve the SNR in Rayleigh-based OTDR system has been demonstrated by several research groups [32-45] during the last five years.

The key advantage of using FBGs as artificial scattering centers is the ability to control their reflectivity and position. The reflectivity values used in these systems are very low (typically around -40 dB) but still significantly higher than the Rayleigh intensity level in a typical single mode fiber (SMF). The positions of the FBGs are generally equally spaced over the sensing fiber, where the distance between two successive FBGs limits the spatial resolution of the sensor system.

From practical point of view, it can be foreseen that the implementation of FBG-based approaches in field applications may be promoted by fast and affordable on-line writing capabilities of weak fiber Bragg grating arrays into ordinary SMF during drawing [46].

2.1 Operation Principles

Each method proposed in the literature has got its own particularity, especially in terms of the optical phase demodulation scheme. Table 1 summarizes the different schemes of FBG-based DAS systems interrogated by optical time domain reflectometry.

Trying to cover most of these ϕ-OTDR variants, Fig. 2 represents a generic set-up. It basically consists of a light source followed by pulse modulation stage which outputs narrow optical pulses (or pulse pairs in some schemes). After amplification and filtering (elimination of noise from the optical amplifier), pulses are launched into the sensing fiber where the FBG array is inscribed. Prior to the photo-detection and data acquisition, an optical demodulation scheme handles the signal reflected from the sensing fiber. Here, the signal is put in an

appropriate form to extract the phase information contained in the reflected optical power upon detection and signal processing steps.

The signals involved for the situation where only two FBGs are considered in an array are schematically presented in Fig. 2. If the rectangular pulse injected into the FUT has a width W greater than twice the separation L between FBG_N and $FBG_{(N+1)}$, the signals reflected from both FBGs overlap in a zone of length $W/2$-L of the ϕ-OTDR trace [42]. If a laser source of narrow linewidth is used (there are a couple of exceptions in the literature where low/medium coherence sources are implemented, cf. Table 1), interference occurs between reflected signals. Let us focus on one of these interference sections, $IF_{N\&N+1}$ created by the superposition of the electric fields $\mathbf{E}_N$ and $\mathbf{E}_{N+1}$ (i.e. optical signals reflected from FBG_N and FBG_{N+1}). The complex reflection coefficient, $\mathbf{r}_N$, and the complex transmission coefficient $\mathbf{t}_N$ for FBG_N are determined as a function of known parameters, namely grating length, grating pitch, and average refractive index modulation [47].

The power level corresponding to $IF_{N\&N+1}$ region can be calculated as

$$P_{N\&(N+1)} = (\boldsymbol{E}_N + \boldsymbol{E}_{N+1})(\boldsymbol{E}_N + \boldsymbol{E}_{N+1})^* = |\boldsymbol{E}_N|^2 + |\boldsymbol{E}_{N+1}|^2 + P_{AC}\cos(\Delta\phi(t) + \theta(t)) \quad (1)$$

where $\theta(t) = \arg(\boldsymbol{r}_{N+1}(t)/\boldsymbol{r}_N(t))$, $\Delta\phi(t)$ is twice the phase difference between FBG_N and FBG_{N+1}, and $P_{AC} = 2|\boldsymbol{E}_N||\boldsymbol{E}_{N+1}|$. The phase component ($\Delta\phi(t)$), indeed carries useful information as it will be modulated when a perturbation is applied on the fiber section between two FBGs [48].

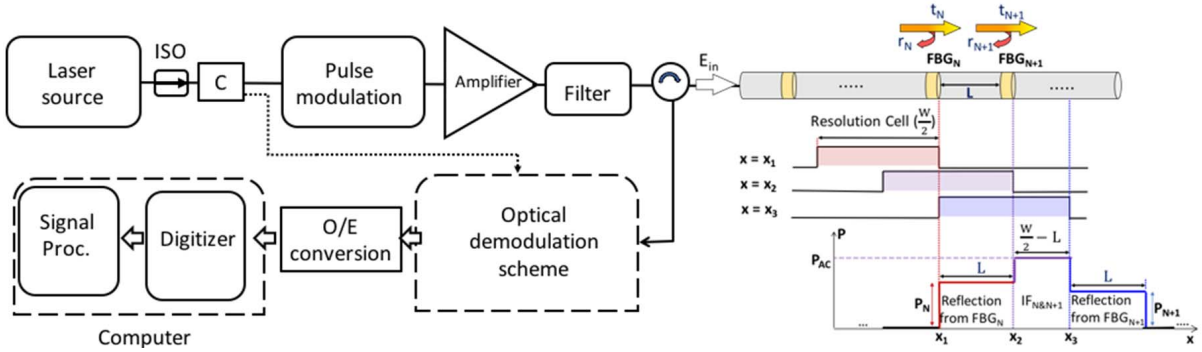

Figure 2. Scheme of a generic interrogator set-up based on ϕ-OTDR and theoretical analysis of reflected signals from a single FBG pair, including power levels of the corresponding φ-OTDR signature. $\boldsymbol{E}_{in}$: complex electric field at the Fiber Under Test (FUT) input.

2.2 Multi-reflection and spectral shadowing crosstalk

In spite of the critical importance of SNR improvement, there are some complications that accompany by the use of equidistant cascaded FBGs. These issues, namely multi reflection crosstalk (MRC) and spectral shadowing crosstalk (SSC) should be taken into account to be able to determine the realistic overall performance parameters of the system.

In addition to the Phase-OTDR signature comprising the signal components given in (1), many possible paths of the interrogating pulse can be found which, after having been subject to multiple reflections (3 reflections, 5 reflections, …), arrive at the same time as the useful signal. The total number of such paths contributing to multi-reflection crosstalk signal can be calculated for 3-reflection and 5-reflection cases, by equations (2) and (3), respectively:

$$M_3(N) = \sum_{i=2}^{N-1}(i-1) \quad (2)$$

$$M_5(N) = \sum_{k=1}^{N-3}\sum_{i=2}^{N-1-k}\left(ki + \sum_{j=1}^{k}(j-2)\right) \quad (3)$$

The MRC effect has been studied in terms of SNR analysis to calculate the longest achievable distance [37].

Spectral shadowing crosstalk effect is another limiting factor cascaded sensor interrogation systems. The interrogating light needs to pass all upstream FBGs (hence carrying the spectral features of all the previous ones) to reach a specific FBG. *de Miguel Soto et al*. proposed and experimentally demonstrated a method to compensate SSC by using a sensor fiber containing four identical FBGs [42]. The compensation can be made since the power terms of the three sections in equation (1) all include the same factor, namely the product of the transmission coefficients of the preceding FBGs in which the spectral properties of these FBGs are hidden [42]. The phase component is then reduced to an expression only depending on the three power levels (represented as P_N, P_{AC}, and P_{N+1} in Fig. 2) which can be read out from the ϕ-OTDR trace.

Recently, we have shown by the way of simulations that these two phenomena (SSC and MRC) being interrelated, the combined effects of SSC and MRC should be analyzed together for the cascaded FBGs, rather

than treating only the signal power in MRC analysis [49]. This is because, in addition to the primary shadowing components due to the interrogating optical pulse passing through all upstream FBGs before reaching a specific FBG, the multi-reflection signals also carry supplementary frequency components (secondary spectral shadowing frequencies) impinged on the actual signal to be measured. Simulations on various test scenarios showed that appearance of ϕ-OTDR trace is drastically influenced by the secondary SSC components making the determination of real frequency content at a particular position a highly challenging task [49].

2.3 Application areas and perspectives

Many market analysis reports agree on similar expectations about the global DAS market size, pronouncing a market value of between $ 700 million to $ 2bn by 2025 [50]. This is largely due to new emerging application fields such as formation of massive acoustic imaging [51], monitoring of transportation infrastructure/railways [52], cracks detection [53], electrical discharge localisation [54], and seismic acquisition (e.g. earthquake identification and localisation [55, 56], crustal structural features detection imaging [55], monitoring of groundwater level [56]).

3. CONCLUSIONS

Fiber-optic distributed acoustic sensing techniques embrace two approaches. Transforming currently installed fiber-optic networks into distributed acoustic sensing arrays has been the main idea behind most of the aforementioned field demonstrations [51- 56]. As an alternative to this approach based on the measurement of Rayleigh backscattering signal, the efforts to modify/improve the sensing fiber has also been attracting a great attention [22-45]. We provide a review of the existing solutions based on FBG array to provide improved sensitivity [32-45]. We emphasize that the multi reflection crosstalk and spectral shadowing crosstalk should be carefully taken into account when designing such systems, making otherwise the interpretation of the measurement results a challenging task [42, 48, 49].

Table 1. Comparison of different schemes of FBG-based DAS interrogated by phase sensitive OTDR.

FBG parameters	Demodulation scheme	SR/ measurement range	Frequency range	Performance parameters	Optical source	Comment	Year	Ref.
R≈ 0.08%, 500 FBGs, L = 2m.	Balanced Michelson interferometer and 3×3 coupler.	5m / 1 km	450-600 Hz	Acoustic phase sensitivity: -158 dB	DFB –LD, linewidth= 5kHz	Demonstrated for underwater acoustic sensing. Use of low cost DFB laser.	2015	[32]
R= -20 dB, 5 FBGs, L = 2m.	Direct detection, Phase unwrapping.	2m / 5 km	5-10 Hz (theoretical max. 500 Hz)	Strain sensitivity: 42.6 nε/rad Error: 6.2 nε (deviation from calibrated system)	TLS (optical freq. swept over 70 MHz) (P =10 dBm, EDFA output) linewidth: 3.7 kHz	MRC analysed. Max detectable frequency is limited by laser sweep time.	2015	[33]
R= -20 dB, 3 FBGs, L = 50m.	Direct detection (RBS), Heterodyne coherent detection (FBG array).	4m / 5km (SR determined by RBS)	Max. 100 Hz	Not quantified.	TLS (step frequency modulation, slow process) linewidth: 3.7 kHz	Combination of ordinary ϕ-OTDR with FBG array. Ordinary ϕ-OTDR is for localization. FBG sensors for dynamic strain.	2016	[34]
R= - 35dB to - 40 dB, 3 FBGs, L= tens of meters	Coherent detection (RBS), Unbalanced 3×3 coupler & Table-look-up scheme (FBG array).	10m / 2.5 km (SR determined by RBS)	50 Hz- 2 kHz	Sensitivity (fiber length variation): 117 pm/$(Hz)^{1/2}$ SNR=56 dB	TLS (P=7 dBm, EDFA output: 21 dBm)	Ordinary ϕ-OTDR is for localization. FBG sensors for dynamic strain measurement.	2017	[35]
R= - 40 dB, 660 FBGs, L= 2.5 m.	Low coherence Michelson interferometer.	2.5 m / 10km	100 Hz- 1kHz	Comparable performance with electrical geophone	Low coherence ASE source	Perspective: surface, sea bed, downhole resource detection.	2017	[36]
R = - 40 dB, 88 FBGs, L = 50 m.	Double pulse, Direct detection. No phase info (quantification is not provided).	50m / 4.5km	3 Hz- 9 kHz	Not reported	Narrow linewidth laser (NLL) Linewidth: 1 kHz (P= 8 dBm, pulse peak power)	RBS generated from the useless part of a single pulse is eliminated. SNR analysis provided in the presence of MRC and RBS.	2017	[37]

FBG parameters	Demodulation scheme	SR/ measurement range	Frequency range	Performance parameters	Optical source	Comment	Year	Ref.
R = - 40 dB, 342 FBGs, L = 2.5 m.	Optical filter (0.1 nm of BW) used to convert wavelength variation to intensity variation.	2.5m / 855 m	2 kHz	Strain measurement resolution 222 nε	Broadband source (filtered to have 7 nm of BW and modulated into ns-pulse)	A reference channel (having reference filter) is used to compensate intensity fluctuations.	2017	[38]
R = -37 dB, 5 FBGs, L = 10 m.	Coherent detection, polarisation diversity scheme.	10m / 20 km	10 Hz- 2.5 kHz	Sensitivity: 3.84 pε/(Hz)$^{1/2}$	NLL Linewidth: 1 kHz (P= 16 dBm)	Phase noise compensation provided (using a reference interferometer).	2018	[39]
R= -40 dB, 964 FBGs, L = 2m.	Static strain: Edge filtering, Dynamic strain: Mach-Zehnder IF and 3×3 coupler	NA / 2 km	DC-12.5 kHz	Dynamic strain sensing in nε scale (max error 3 nε) 1 με resolution for static strain.	DFB-LD, Linewidth: 10 MHz	Pulses at two different wavelengths are time interleaved. Use of low cost DFB laser.	2018	[40]
R= -40 dB, 332 FBGs, L = 3m.	Mach-Zehnder IF and 3×3 coupler.	3m / 1 km	10 Hz- 25 kHz	SNR = 6.7 dB Max. error 3.4 nε.	DFB-LD, Linewidth: 10 MHz	Use of low cost DFB laser.	2018	[41]
R ≈ 0.02%, 4 FBGs, L = 5m.	Direct detection. No phase info (vibration quantification is not provided).	5m / 2.5 km	2 kHz (theory up to 10 kHz)	Spectral shadowing compensated.	Ultra-NLL Linewidth: 0.1 kHz	Spectral shadowing suppression method proposed and implemented.	2019	[42]
R= - 40 dB, 88 FBGs, L = 50m.	Double-pulse and heterodyne coherent detection.	50m / 4.5 km	0.2 Hz	18 dB SNR improvement compared to RBS. The influence of laser frequency drift reduced.	NLL	Very low frequency measurement. Both sinusoidal and triangular signals demodulated.	2018	[43]
R= -43 dB, 200 FBGs, L = 5m.	Scalable homodyne demodulation and PGCD-CM(1) algorithm.	5m / 1 km	2.5 kHz	SNR = 34.5 dB Capability of measuring slow drifts and fast vibration.	Tunable laser, Linewidth: 200 kHz	Phase unwrapping is not needed.	2019	[44]
R= - 40 dB, 51 FBGs, L = 10 m.	Self-heterodyne detection. Two pulses used (frequency shifts of 150 and 80 MHz).	11.7m / 42 km	8 Hz- 1 kHz	Max. error 1.32 nε.	Linewidth: 3.7 kHz	Raman distributed amplifying employed.	2019	[45]

(1): PGCD-CM: Phase-Generated Carrier Differentiate and Cross-Multiply.

ACKNOWLEDGEMENTS

Kivilcim Yüksel gratefully acknowledges financial support from the TUBITAK (BIDEB-2219-1059B191600612). Manuel Lopez-Amo Sainz acknowledges Spanish AEI project TEC2016-76021-C2 and FEDER Funds.

REFERENCES

[1] A. Hartog: Distributed fiber-optic sensors: Principles and applications, in *Optical Fiber Sensor Technology,* G.T.V. Grattan and B.T. Meggitt, Ed., Kluwer Academic Publishers, 2000.
[2] M. Wuilpart: Rayleigh scattering in optical fibers and applications to distributed measurements, in *Advanced Fiber Optics: Concepts and Technology*, L. Thevenaz, EPFL Press /CRC, 2011.
[3] J. C. Juarez *et al*.: Distributed fiber-optic intrusion sensor system, *J. Lightwave Technol*., vol. 23, pp. 2081-2087, 2005.
[4] Y. Lu *et al*.: Distributed vibration sensor based on coherent detection of phase-OTDR, *J. Lightwave Technol*., vol. 28, pp. 3243–3249, Nov. 2010.
[5] Z. Pan, K. Liang, Q. Ye, H. Cai, R. Qu, and Z. Fang: Phase-sensitive OTDR system based on digital coherent detection, in *Proc. ACP*, Shanghai, China, Nov. 2011.
[6] K. Y. Aldogan *et al*.: Development of a phase-OTDR interrogator based on coherent detection scheme, *Uludag University J. of The Faculty of Engineering*. vol. 23, pp. 370-355 2018.
[7] H. He *et al*.: Self-mixing demodulation for coherent phase-sensitive OTDR system, *Sensors*, vol. 16, 681, May 2016.
[8] M. Yu *et al*.: Phase-sensitive optical time-domain reflectometric system based on a single-source dual heterodyne detection scheme, *Appl. Opt*., vol. 56. pp. 4058-4064, May 2017.
[9] A. Masoudi *et al*.: Analysis of distributed optical fibre acoustic sensors through numerical modelling, *Opt. Express*, vol. 25, pp. 32021-32040, Dec. 2017.

[10] X. He *et al*.: Multi-event waveform-retrieved distributed optical fiber acoustic sensor using dual-pulse heterodyne phase-sensitive OTDR, *Opt. Lett.,* vol. 42, pp. 442–445, Feb. 2017.

[11] H. He *et al*.: Enhanced range of the dynamic strain measurement in phase-sensitive OTDR with tunable sensitivity, *Opt. Express*, vol. 28, pp. 226-237, Jan. 2020.

[12] Z. Qin *et al*.: Wavelet denoising method for improving detection performance of distributed vibration sensor, *IEEE Photonics Technol. Lett*., vol. 24, pp. 542-544, Apr. 2012.

[13] T. Zhu et al.: Enhancement of SNR and spatial resolution in ϕ-OTDR system by using two-dimensional edge detection method, *J. Lightwave Technol*., vol. 31, pp. 2851-2856, Sep. 2013.

[14] A. E. Alekseev *et al*.: A phase-sensitive optical time-domain reflectometer with dual-pulse diverse frequency probe signal, *Laser Phys.*, vol. 25, 115106, 2015.

[15] H. Yue *et al*.: Simultaneous and signal-to-noise ratio enhancement extraction of vibration location and frequency information in phase-sensitive optical time domain reflectometry distributed sensing system, *Opt. Eng*., vol. 54, Apr. 2015.

[16] X. Hui *et al*.: Hilbert–Huang transform time-frequency analysis in ϕ-OTDR distributed sensor, *IEEE Photonics Technol. Lett*., vol. 26. pp. 2403-2406, Dec. 2014.

[17] I. Olcer *et al*.: Adaptive temporal matched filtering for noise suppression in fiber optic distributed acoustic sensing, *Sensors*, vol. 17, 1288, Mar. 2017.

[18] Z. Pan, K. Liang, J. Zhou, Q. Ye, H. Cai, and R. Qu: Interference-fading-free phase-demodulated OTDR system, in *Proc. OFS*, Beijing, China, Oct. 2012.

[19] D. Chen *et al*.: High-fidelity distributed fiber-optic acoustic sensor with fading noise suppressed and sub-meter spatial resolution, *Opt. Express*, vol. 26. pp. 16138-16146, Jun. 2018.

[20] Y. Wu *et al*.: Interference fading elimination with single rectangular pulse in ϕ-OTDR, *J. Lightwave Technol*., vol. 37, pp. 3381-3387, July 2019.

[21] Y. Wang *et al*.: Optical fiber vibration sensor using least mean square error algorithm, *Sensors*, vol. 20, 2000, Mar. 2020.

[22] S. Loranger *et al*.: Rayleigh scatter based order of magnitude increase in distributed temperature and strain sensing by simple UV exposure of optical fibre, *Sci. Rep.*, vol. 5, 11177, June 2015.

[23] Y. Xu *et al*.: Optical fiber random grating-based multiparameter sensor, *Opt. Lett*., vol. 40, pp. 5514–5517, Nov. 2015.

[24] A. Yan *et al*.: Distributed optical fiber sensors with ultrafast laser enhanced Rayleigh backscattering profiles for real-time monitoring of solid oxide fuel cell operations, *Sci. Rep.*, vol. 7, no. 1, 9360, 2017.

[25] P. S. Westbrook, K. S. Feder, R. M. Ortiz, T. Kremp, E. M. Monberg, H. Wu, D. A. Simo, and S. Shenk: Kilometer length low loss enhanced back scattering fiber for distributed sensing, in *25th Int. Conference on Optical Fiber Sensors,* 2017, p. 17012426.

[26] J. Jason, S. M. Popov, O. V. Butov, Y. K. Chamorovskiy, K. M. Golant, A. A. Fotiadi, and M. Wuilpart: Sensitivity of high Rayleigh scattering fiber in acoustic/vibration sensing using phase-OTDR, *Proc. of SPIE*, vol. 10680, 2018, 106801B-1.

[27] G. Cedilnik *et al*.: Pushing the reach of fiber distributed acoustic sensing to 125 km without the use of amplification, *IEEE Sens. Lett.*, vol. 3, pp. 1-4 , 2019.

[28] A. Donko, R. Sandoghchi, A. Masoudi, M. Beresna, and G. Brambilla: Low-loss micro-machined fiber with rayleigh backscattering enhanced by two orders of magnitude, in *Proc. 26th Int. Conference on Optical Fiber Sensors*, Lausanne, Switzerland, 24–28 Sep. 2018.

[29] K. Hicke *et al.:* Enhanced distributed fiber optic vibration sensing and simultaneous temperature gradient sensing using traditional C-OTDR and structured fiber with scattering dots, *Sensors*, vol. 19, Sep. 2019.

[30] B. Redding *et al*.: Low-noise distributed acoustic sensing using enhanced backscattering fiber with ultra-low-loss point reflectors, *Optics Express*, vol. 28, May 2020.

[31] H. Li *et al*.: Ultra-high sensitive quasi-distributed acoustic sensor based on coherent OTDR and cylindrical transducer, *J. Lightwave Technol*., vol. 38, pp. 929-938, Feb. 2020.

[32] C. Wang *et al*.: Distributed OTDR-interferometric sensing network with identical ultra-weak fiber Bragg gratings, *Opt. Express*, vol. 23. pp. 29038-29046, Oct. 2015.

[33] F. Zhu *et al*.: Improved ϕ-OTDR sensing system for high-precision dynamic strain measurement based on ultra-weak fiber Bragg grating array, *J. Lightwave Technol*., vol. 33. pp. 4775-4780, Dec. 2015.

[34] X. Zhang *et al*.: Enhanced ϕ-OTDR system for quantitative strain measurement based on ultra-weak fiber Bragg grating array, *Opt. Eng.,* vol. 55, 054103, May 2016.

[35] X. Zhang *et al*.: A high performance distributed optical fiber sensor based on ϕ-OTDR for dynamic strain measurement, *IEEE Photonics J*., vol. 9, 6802412, May 2017.

[36] J. Tang, L. Li, H. Guo, H. Yu, H. Wen, and M. Yang: Distributed acoustic sensing system based on continuous wide-band ultra-weak fiber Bragg grating array, in *Proc. OFS*, Jeju, Korea, Apr. 2017.

[37] T. Liu *et al*.: Phase sensitive distributed vibration sensing based on ultra-weak fiber Bragg grating array using double-pulse, *Opt. Eng*., vol. 56, 084104, Aug. 2017.

[38] P. Han *et al*.: A high-speed distributed ultra-weak FBG sensing system with high resolution, *IEEE Photonics Technol. Lett*., vol.29, pp. 1249-1252, Aug. 2017

[39] M. Wu *et al*.: Highly sensitive quasi-distributed fiber-optic acoustic sensing system by interrogating a weak reflector array, *Optics Letters*, vol. 43, pp. 3594-3597, Jul. 2018.

[40] Z. Li *et al*.: Simultaneous distributed static and dynamic sensing based on ultra-short fiber Bragg gratings, *Opt. Express*, vol. 26. pp. 17437-17446, Jun. 2018.

[41] Y. Tong *et al*.: High-speed Mach-Zehnder-OTDR distributed optical fiber vibration sensor using medium-coherence laser, *Photonic Sensors*, vol. 8, pp. 203-212, 2018.

[42] V. de Miguel Soto *et al*.: Spectral shadowing suppression technique in phase-OTDR sensing based on weak fiber Bragg grating array, *Opt. Lett.,* vol. 44. pp. 526-529, Feb. 2019.
[43] T. Liu *et al*.: Interrogation of ultra-weak FBG array using double-pulse and heterodyne detection, *IEEE Photonics Technol. Lett*., vol. 30. pp. 677-680, Apr. 2018.
[44] Y. Muanenda *et al*.: Dynamic phase extraction in high-SNR DAS based on UWFBGs without phase unwrapping using scalable homodyne demodulation in direct detection, *Opt. Express*, vol. 27. pp. 10644-10658, Apr. 2019.
[45] Y. Shan *et al*.: An enhanced distributed acoustic sensor based on UWFBG and self-heterodyne detection, *J. Lightwave Technol*., vol. 37. pp. 2700-2705, Jun. 2019.
[46] H. Y. Guo *et.al*.: Online writing weak fiber Bragg gratings array, *Chin. Opt. Lett*., vol. 11, 030602, 2013.
[47] T. Erdogan: Fiber grating spectra, *J. Lightwave Technol*., vol. 15, pp. 1277-1294, 1997.
[48] K. Yüksel, J. Jason, V. De M. Soto, M. Lopez-Amo, P. Megret, and M. Wuilpart: Performance evaluation of phase-OTDR sensing system based on weak fiber Bragg grating array, in *Proc. IEEE Photonics Benelux Chapter Annual Symposium* , Brussels, Belgium, Nov. 2018.
[49] E. B. Kocal, K. Yüksel, and M. Wuilpart: Combined effect of multi-reflection and spectral shadowing crosstalk in phase-OTDR system using fiber Bragg gratings, *International Conference on Optical Fiber Sensors OFS 2020*, The Westin Alexandria, Virginia, USA (accepted).
[50] Persistence Market Research, "Global Distributed Acoustic Sensing Market to Surpass US$ 2 Billion in Revenues by 2025," http://www.persistencemarketresearch.com/mediarelease/distributed-acoustic-sensing- market.asp.
[51] T. Parker *et al*.: Distributed acoustic sensing – A new tool for seismic applications, *First Break*, vol. 32. pp. 61-69, Feb. 2014.
[52] Z. Wang, B. Lu, H. Zheng, Q. Ye, Z. Pan, H. Cai, R. Qu, Z. Fang, and H. Zhao: Novel railway-subgrade vibration monitoring technology using phase-sensitive OTDR, in *Proc. OFS*, Jeju, Korea, Apr. 2017.
[53] X. Chapeleau *et al*.: Assessment of cracks detection in pavement by a distributed fiber optic sensing technology, *J. Civ. Struct. Health Monit*., vol. 7. pp. 1-12, Aug. 2017.
[54] G. Ma *et al*.: A non-intrusive electrical discharge localization method for gas insulated line based on phase-sensitive OTDR and Michelson interferometer, *IEEE Transactions on Power Delivery*, vol. 34. pp. 1324-1331, Aug. 2019.
[55] P. Jousset *et al*.: Dynamic strain determination using fibre-optic cables allows imaging of seismological and structural features, *Nature Communications*, vol. 9, Jul. 2018.
[56] J. B. Ajo-Franklin *et al*: Distributed acoustic sensing using dark fiber for near-surface characterization and broadband seismic event detection, *Scientific Reports*, vol. 9, Feb. 2019.